{bold {ital In situ}} video observation of 180Â° domain switching in LiTaOâ by electro-optic imaging microscopy

ARTICLE *in* JOURNAL OF APPLIED PHYSICS · FEBRUARY 1999

Impact Factor: 2.18 · DOI: 10.1063/1.369542

2 AUTHORS, INCLUDING:

Terence E. Mitchell
Los Alamos National Laboratory
378 PUBLICATIONS **6,542** CITATIONS

In situ video observation of 180° domain switching in LiTaO3 by electro-optic imaging microscopy

Venkatraman Gopalan and Terence E. Mitchell

Citation: J. Appl. Phys. **85**, 2304 (1999); doi: 10.1063/1.369542
View online: http://dx.doi.org/10.1063/1.369542
View Table of Contents: http://jap.aip.org/resource/1/JAPIAU/v85/i4
Published by the AIP Publishing LLC.

In situ video observation of 180° domain switching in $LiTaO_3$ by electro-optic imaging microscopy

Venkatraman Gopalan[a)]
Materials Research Laboratory, Pennsylvania State University, University Park, Pennsylvania 16802

Terence E. Mitchell
Center for Materials Science, Los Alamos National Laboratory, Los Alamos, New Mexico 87545

(Received 27 August 1998; accepted for publication 12 November 1998)

We report video observation of 180° domain switching in congruent $LiTaO_3$ under an external electric field by electro-optic imaging microscopy. The sideways wall velocity of independently growing 180° domains in the *Z* plane of the crystal was measured to be 0.1–0.2 mm/s at a constant field of 21.2 kV/mm. The merging of independently growing domains results in a serrated domain front which displays an order of magnitude increase in the wall velocity to ~2.3 mm/s. We show that this is directly related to ledge formation upon domain merging where preferential nucleation takes place. These velocities are also an order of magnitude higher than those reported earlier for equivalent switching times that were measured by pulsed voltage application followed by *ex situ* optical observation. © *1999 American Institute of Physics.* [S0021-8979(99)05004-5]

I. INTRODUCTION

Lithium tantalate along with lithium niobate are presently key materials in integrated optics,[1] surface acoustic wave devices,[2] and holography.[3] Despite their being known for many decades, studies on domain kinetics in these materials have only recently been done.[4] This is partly due to the realization of the possibility of domain reversal at room temperature despite very large coercive fields in the congruent crystals of these materials (~21 kV/mm) and partly due to the discovery that 180° domain walls introduce birefringence near the walls which facilitates imaging of the domains by *nondestructive* light microscopy.[5]

The previous studies on domain kinetics in $LiTaO_3$ have performed partly *ex situ* in the sense that constant voltage pulses were applied to the crystal to nucleate and grow domains, and the evolution process was separately monitored after every pulse by optical observation under a light microscope.[4] The electrical field application and optical observation steps were separate. As we will show here, this *ex situ* technique underestimates the wall velocities by an order of magnitude. This has serious implications for the domain wall mobility data measured by pulse voltage experiments reported in the literature for many ferroelectrics.[6–8] The second important phenomenon which has escaped careful observation by pulse voltage experiments is that the merging of sideways growing domains results in an order of magnitude increase in the velocity of the serrated domain wall front that forms upon the merger.

This study addresses both these important issues. By using real-time electro-optic imaging microscopy, the constant voltage applied throughout the nucleation, growth, and merger of domains provides a contrast at the 180° walls through the electro-optic effect which is recorded on video. Important too, it also eliminates having to apply pulse voltages to arrest domain growth for *ex situ* observation, thus eliminating possible reversible domain motion or pinning. The imaging also relies on the index difference at a domain wall due to the electro-optic effect, which is nondestructive, unlike the acid etch techniques used previously.[6–8] By analyzing the video data frame by frame, one can also monitor the kinetics of merging domains.

This article is organized as follows. Electro-optic imaging microscopy (EOIM) is discussed in Sect. II. In Sec. III the experimental domain kinetics data in $LiTaO_3$ are presented. Finally, in Sec. IV there is a discussion of the results followed by conclusions in Sec. V.

II. ELECTRO-OPTIC IMAGING MICROSCOPY

The electro-optic effect in a noncentrosymmetric crystal structure produces a refractive index change (n_{ij}) in the material in response to an externally applied electric field (E_k) as follows:

$$\Delta\left(\frac{1}{n_{ij}^2}\right)=r_{ijk}E_k. \tag{1}$$

Since the electro-optic coefficients, r_{ijk}, form a tensor, the index change is dependent on the orientation of the crystal with respect to an applied electric field. As an example, let us consider a 180° ferroelectric domain wall in a uniaxial crystal such as $LiTaO_3$ ($3m$, C_{3v}), as shown in the schematic of Fig. 1. Under a uniform electric field *E*, the refractive index in one domain increases from $n \Rightarrow n+\Delta n$, while it decreases in the other from $n \Rightarrow n-\Delta n$, thus providing an index contrast across the domain wall. In $LiTaO_3$, $r_{113}=r_{223}\sim 8.4$ pm/V (at 633 nm)[9] and, therefore, under a field E_3 ~21 kV/mm (the coercive field of congruent $LiTaO_3$) in the *z* direction, one obtains a $\Delta n_{11}=\Delta n_{22}=9.1\times 10^{-4}$, where the index increases in the domain where the external field is antiparallel to the direction of spontaneous polarization. Since the domain wall in congruent $LiTaO_3$ is perpendicular

a)Electronic mail: vgopalan@psu.edu

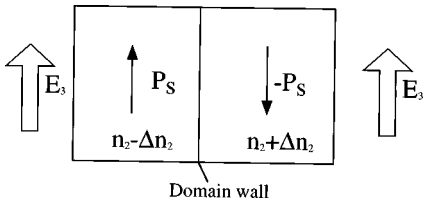

FIG. 1. Schematic showing the principle of electro-optic imaging at a 180° ferroelectric domain wall with spontaneous polarizations, P_s and $-P_s$ across the wall. A uniform external electric field E applied across the wall in $LiTaO_3$ changes the ordinary refractive index (n_0) of the domain to $\Delta n_{22} = -(1/2)n_0^3 r_{223} E_3$ where r_{223} is the electro-optic coefficient and E_3 is the field applied along the polarization axis. The index increases when E_3 is antiparallel to P_s and decreases when E_3 is parallel to P_s.

to the crystallographic y direction, when one crosses the domain wall, this index difference Δn_{22} at the wall will cause scattering of the transmitted light in the crystal. This can be used to image a domain wall though the crystal thickness in a Z-cut crystal under an optical microscope without any polarizers.

We would like to note that, in addition to this contrast mechanism, we have also observed birefringence ($n_{11} - n_{22}$) at the domain walls in congruent $LiTaO_3$ even without the presence of any external electric field[5] which we have shown to be related to the presence of internal fields[5] and therefore to the lithium nonstoichiometry of the crystals.[10] This birefringence cannot be obtained from the linear electro-optic effect since $r_{13}=r_{23}$. When the internal field is parallel to the polarization (the preferred orientation) on one side of the domain wall and antiparallel to the polarization (frustrated state) on the other side,[5] it tends to distort the lattice at the domain wall resulting in local strains, in-plane electric fields (E_2 along the y axis), and optical birefringence ($n_{11}-n_{22}$).[11,12] It can be shown that a combination of electrostriction, photoelasticity, and the quadratic electro-optic effect will give rise to birefringence ($n_{11}-n_{22}$) which has cross terms proportional to E_2E_3.[12] Since E_2 at the walls is now nonzero, an applied field E_3 along the z axis can increase or decrease the birefringence at the wall linearly, which has also been observed using near-field scanning optical microscopy.[13]

In any case, the domain walls studied here in congruent $LiTaO_3$ are visible in plain transmitted light, both with and without cross polarizers, and both with and without external electric field E_3. However, the presence of a Nomarski slider

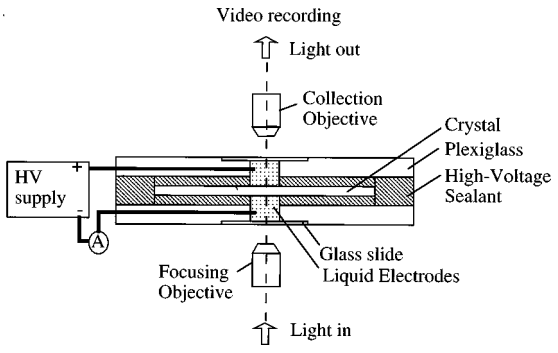

FIG. 2. Schematic of the electro-optic imaging microscopy setup.

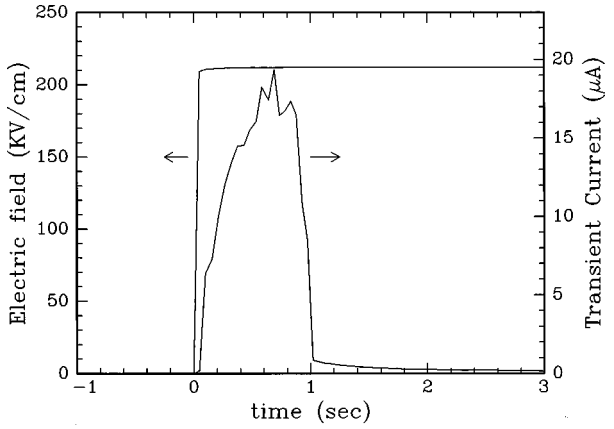

FIG. 3. Applied voltage pulse and transient current response of congruent Z-cut $LiTaO_3$ crystal.

(also called differential interference contrast) along with cross polarizers considerably improves this contrast. Using this contrast mechanism, one can directly study the movement of 180° domains in ferroelectric $LiTaO_3$ under an external electric field. The schematic of our electro-optic imaging setup is shown in Fig. 2. An electric field was applied to the sample using a saturated KNO_3 solution in water across the faces of Z-cut $LiTaO_3$ crystals of congruent composition obtained from Yamaju Ceramics, Inc. Japan. Details of the transient current measurement upon domain inversion and calculation of the spontaneous polarization, P_s, have been reported earlier.[5] In this study, the holder for applying voltage was specially designed to trap the liquid electrode columns on either side of the crystal with transparent glass slides. The entire holder assembly can be easily inserted into a regular optical microscope in transmission mode, where light propagates through the first glass slide, the liquid electrode, the crystal, the second liquid electrode, and the second glass slide in succession, before being collected by a 4× objective. The electrode area was a circle 4 mm in diameter. However, the imaging area on the video screen after magnification was only 0.97×0.73 mm square and was situated at the center of the electrode area. The imaging was performed in transmission mode using cross polarizers in combination with a Nomarski objective. With this setup, the transient current measurement during domain reversal and optical observation of the evolving domain structures were monitored simultaneously. The video recording was performed with a digital camera and a regular VCR with 30 frames per second. The film recorded was digitized using a video card and software on a Power Macintosh, through which every frame could be extracted. The final resolution was an ~6×6 μm pixel size and a 160×120 pixel image space.

III. 180° DOMAIN KINETICS

A. Transient current and video data

Using the electro-optic imaging microscope, we monitored the evolution of 180° domains in congruent $LiTaO_3$ crystals. Information on the polarization hysteresis and domain kinetics on 180° domains by pulse voltage application has recently been reported in detail.[4] The coercive field of

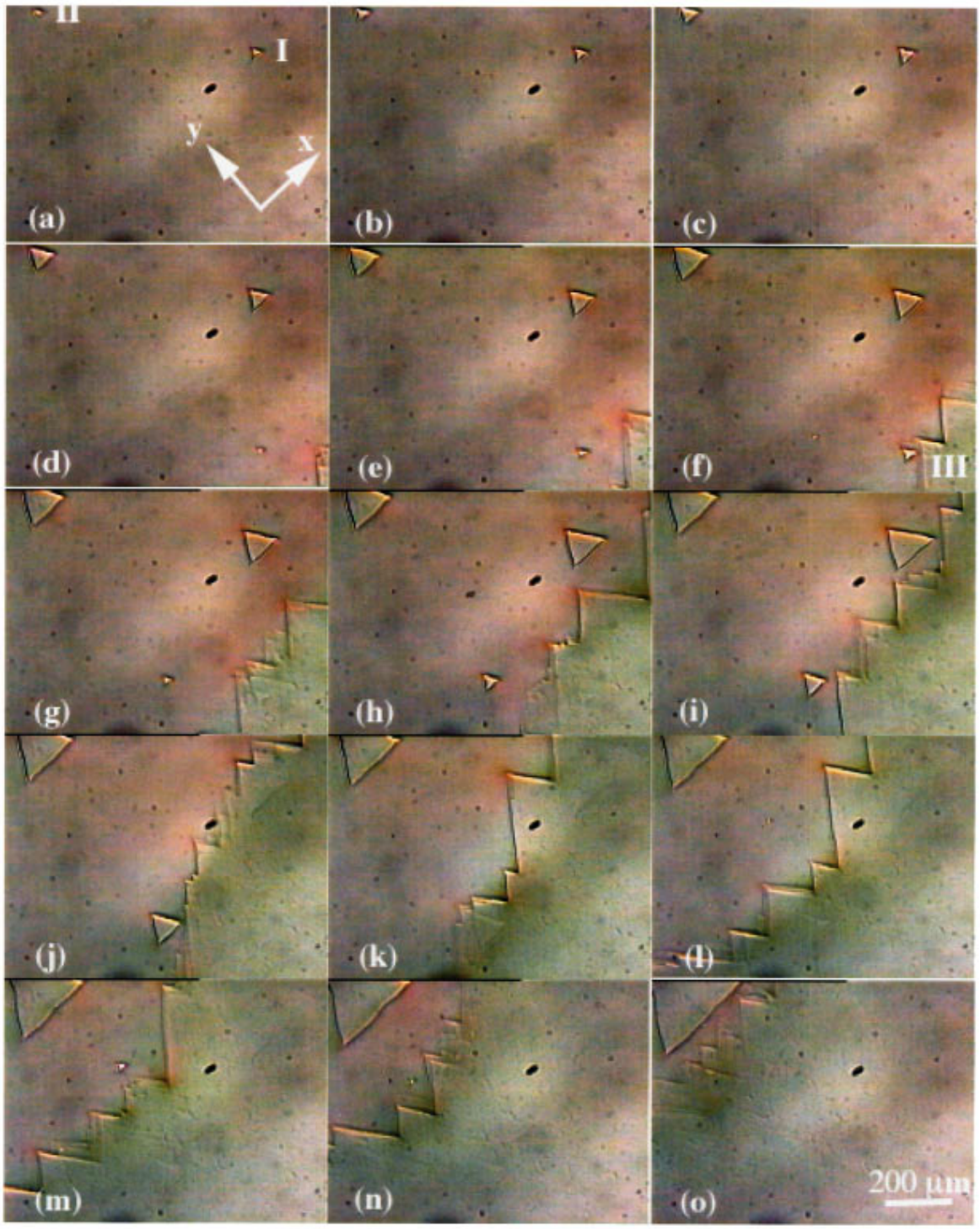

FIG. 4. Selected video frames from *in situ* recording of the nucleation and growth of 180° domains in congruent $LiTaO_3$ under an external field of 212 kV/cm (applied at time $t=0$) using EOIM. Frame (a) corresponds to $t=0.5$ s, and all successive frames [(b)–(o)] are 1/30 s apart from each other. The polarization axes are normal to the plane of the figure (the Z plane), and the crystallographic x and y axes are marked.

the crystals used in this study was ~20.7 kV/mm. In this article, we report results on one constant field of $E=21.2$ kV/mm applied as a step voltage to the crystal. The resultant transient current response is shown in Fig. 3. The switching time was 1 s.

Figure 4 shows a series of frames obtained from corresponding electro-optic imaging data. If the step voltage were applied at time $t=0$, the first frame [Fig. 4(a)] would correspond to $t=0.5$ s. Every successive frame is spaced by 1/30 s and labeled Figs. 4(b), 4(c), 4(d), etc. The final frame is Fig. 4(o) and corresponds to $t=0.966$ s. The polarization axis is normal to the plane of the image. The 180° domains nucleate and grow in the form of triangular domains with domain walls perpendicular to the mirror plane[5] [for ex-

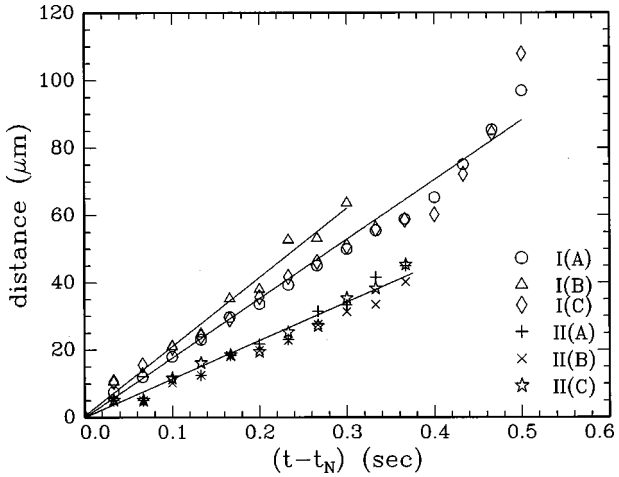

FIG. 5. Sideways growth of sides a, b, and c of domains I and II (see Fig. 4) as a function of time after nucleation at time $t_N=0.4$ s for domain I and $t_N=0.466$ s for domain II. A step voltage of 212 kV/cm was applied at $t=0$.

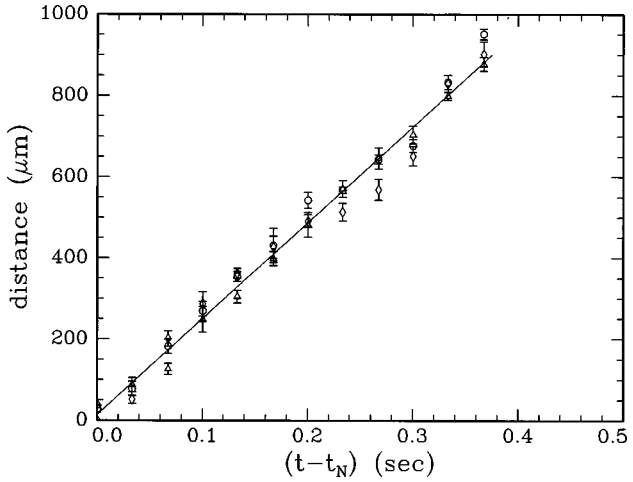

FIG. 6. Sideways growth of merged domain front III in Fig. 4 along the y axis as a function of time after appearing on the screen at time $t_N=0.633$ s. The three different symbols in the data (the circle, triangle, and rhombus) are for three different line scans along the y axis that have different origins.

ample, domains I and II in Fig. 4(a)]. The crystallographic y axis corresponds to [1100] and lies in the mirror plane. Eventually, the domains merge sideways and form a merged domain front like domain III in Fig. 4(f). We will now proceed to analyze the wall mobilities of domains I, II, and II shown in Fig. 4.

B. Sideways wall velocities

Each frame in Fig. 4 is 160 pixels wide and 120 pixels high, with each pixel being 6×6 μm^2. The resolution with which we could estimate the position of the walls was within ~3 pixels. Assigning the bottom left-hand corner of every frame as pixel coordinate $(0,0)$, we determined the origin of domain I as O_{I} $(124,93)$ at a nucleation time, $t_N=0.4$ s and the origin of domain II as O_{II} $(16,112)$ at $t_N=0.466$ s. We label the three domain walls of each of the triangular domains I and II as I(A), I(B), I(C) and II(A), II(B), and II(C). Referring to the crystallographic x and y axes in Fig. 4(a), wall A is perpendicular to the y axis, and B and C follow counterclockwise around the triangle from wall A. The average distance traveled by each of the walls from the origin, O, in a direction normal to the wall was measured and is plotted in Fig. 5. The walls appear to move at a steady state sideways velocity, v_s, which varies from domain to domain. Walls I(A) and I(C) move at a mean velocity of 158 μm/s and I(B) moves at ~206 μm s/s. The mean wall velocities for II(A), II(B), and II(C) are ~114 μm/s. Thus there can be a variation in the wall velocity from domain to domain by a factor of 2.

Domain III [labeled in Fig. 4(f)] is a merged domain wall front which was created out of the field of view of the video recorder and sweeps through the frame. The serrated wall front now has a fine structure comprising vertices of triangles similar to domains I and II with a distribution of length scales. By arbitrarily assigning a pixel origin such as $O_{\mathrm{III}}(157,3)$ and by measuring the distance traveled along the $+y$ crystallographic direction, we can measure the effective sideways velocity of the front in that direction. This was done with three different origins, O_{III}, in order to average the raggedness of the front and the results are shown in Fig. 6. One interesting observation is that the front moves with an effective steady state mean velocity of ~2360 μm/s which is an order of magnitude larger than that for domains I and II. We will address this ''speeding up'' phenomenon on domain merging in Sec. IV.

C. Area fraction of domains with time

The area fractions of domains evolving with time were measured from the video frames in Fig. 4 and are shown for domains I and II in Fig. 7. As expected for equilateral triangles with walls growing out at a steady state velocity, the area fraction (A_{I} and A_{II}) goes quadratically as $A=3\sqrt{3}v_s^2t^2$ with time as shown by the solid line fits, with v_s of 114 and 155 μ/s for domains I and II, respectively.

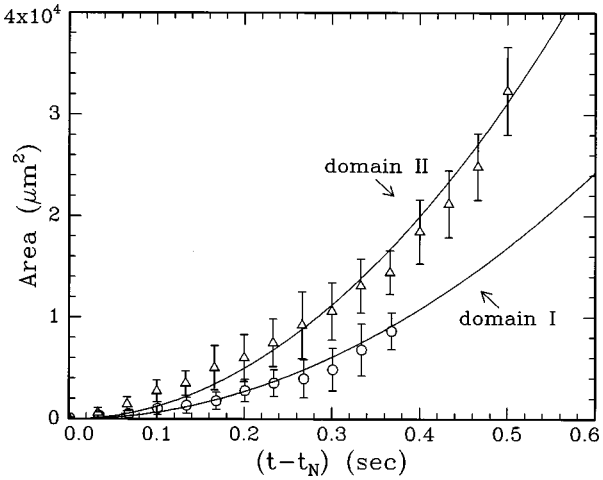

FIG. 7. Area (A) of domains I and II in Fig. 4 as a function of time (t). The solid lines are quadratic fits of the form $A=3\sqrt{3}v_s^2t^2$ where v_s is 114 μm/s for domain I and 155 μm/s for domain II.

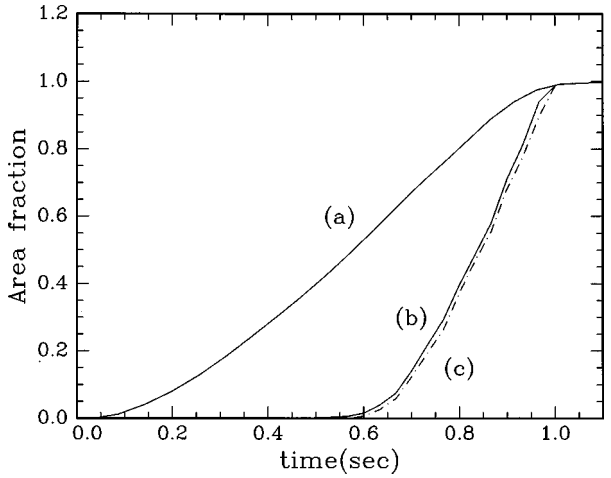

FIG. 8. Area fraction of growing 180° domains resulting from (a) integrating the current pulse of Fig. 3, (b) the total area of growing domains in Fig. 4, and (c) the area fraction of merged domain front III, in Fig. 4 only.

The total area fraction of evolving domains in the video screen with time was experimentally measured and is shown in Fig. 8, as curve (b). The time $t=0$ in this plot is the time when the voltage pulse was applied. Also shown are two other curves. Curve (c) shown by the broken line is the area fraction of the merged domain front (domain III) in Fig. 4. Curve (a) shows the area fraction with time for the entire electrode region (4π mm^2), calculated by integrating the current peak shown in Fig. 3.

Curve (b) for the video data starts ~0.4 s after the application of voltage at $t=0$ s, while curve (a) from current data for the entire electrode region indicates domain growth immediately after the application of voltage. Since the area observed by the video recorder was only a 0.97×0.73 mm^2 area at the center of the electrode which was a circle of 4 mm in diameter, it implies that nucleation of domains started at the electrode periphery (outside the video imaging area) and proceeded inwards. We have observed this in general, i.e., that the nucleation of domains have a slight preference at the electrode edges, which we believe is due to a slightly higher electric field value at the electrode periphery (due to fringing fields) than at the electrode center. Stresses at the electrode edges due to holding may also contribute to a slightly higher nucleation rate at the edges.

The switching time, defined as the start of nucleation to complete domain reversal in the observed area, is ~1 s for the electrode area. It appears to be only ~0.6 s for the video area. The switching time as defined above will decrease as one decreases the area of observation. However, since our video resolution is limited to 6×6 μm s, we cannot determine the exact start of nucleation and hence the switching time for the video area may in fact be longer. Nonetheless, we can assert that the switching time in the video area is dominated by the movement of merged domain front III, as shown by curve (c) which is very close to curve (b) in Fig. 8. It also implies that the influence of domain merging and speeding up of the merged front are dominant towards the end of the switching time.

IV. DISCUSSION

A. Wall velocities

The magnitude of sideways domain wall velocities for independently growing triangular domains is an order of magnitude larger than those reported earlier[4] for $LiTaO_3$ using pulsed voltage experiments. This comparison is made in the following way. The coercive fields vary slightly from wafer to wafer in $LiTaO_3$, without, however, any significant change in the activation energies of the switching times of the sideways wall velocities with the electric field.[4] Therefore, one can compare the sideways wall velocities of two different wafers at equivalent switching times (for similar macroscopic electrode areas) rather than at the same electric field value. For example, in this study on wafer F, the sideways wall velocity is 100–200 μm/s for a switching time of ~1 s. In Ref. 4, for the same switching time of 1 s, the sideways wall velocities were 15 μm/s for wafer A and 10 μm/s for wafer B, which are an order of magnitude smaller. There are two possible reasons for this discrepancy. First, there may be substantial recoil or backtracking of the domain wall at the falling edge of a voltage pulse, resulting in a lower net wall velocity. Second, every time a domain wall has moved to a new position with a voltage pulse and allowed to stabilize for ~1–2 s, moving it again with the next pulse may require an initial incubation period to destabilize it before it reaches its steady state velocity again. We discuss each of these possibilities below.

The primary difference in the sideways wall velocity measurement between this study and that in Ref. 4 is that this study relies on real-time video imaging of growing domains under an electric field applied *in situ*, whereas in Ref. 4, the velocity measurements were made by applying pulses of voltage followed by *ex situ* optical observation. This suggests that the sharp falling edge (<1 ns) of a voltage pulse may result in a partial reversal of domain wall motion. In other words, when the voltage is suddenly removed from across a growing 180° domain, there is an inertial recoil of the domain wall which makes it backtrack. The evidence for such backtracking of a domain wall was reported in Ref. 4, where, below a certain applied pulsewidth, the domain shrinks back completely, independent of the magnitude of applied voltage. This critical pulse width was called stabilization time, and was ~1.5–2 s in congruent $LiTaO_3$.[4] Above this pulse width, one observes net domain growth upon application of a voltage pulse. However, this does not rule out partial recoil of the domain wall even at pulse widths larger than the reported stabilization time, which one is sure to miss in *ex situ* observation. However, keeping in mind that the velocity of recoil is much faster[4] than the original growth velocity, even an *in situ* technique such as electro-optic imaging microscopy can miss recording this recoil if one records with an ordinary 30 frames/s video recorder. This study shows that such backtracking, if present, is significant enough to make an order of magnitude difference in sideways wall velocity measurements. Further, one would also expect that the faster a domain wall moves, the larger the recoil would be under pulse voltage application. Therefore, even the activation fields[4] associated with the exponential

behavior of v_s with electric field E are most likely underestimated in the previous reports made by pulsed voltage experiments.

The other possibility is that between each voltage pulse application there may be enough time for a domain to stabilize through partial relaxation of nonstoichiometric point defect complexes. We have already shown the strong influence of lithium nonstoichiometry on internal fields,[10] domain wall strains,[11,12] stabilization times,[4] and birefringence[5] at domain walls in lithium tantalate crystals. The time gaps between the application of voltage pulses for wall velocity measurements in Ref. 4 were of the order of 5–10 min which is much longer than the stabilization time of ~1–2 s in congruent $LiTaO_3$. It is therefore likely that the elastic and electrostatic relaxation of the lattice near a domain wall may stabilize and partially pin this wall. The next voltage pulse has to first unpin this wall before it can reach its steady state velocity again. Let us call this initial time to accelerate to a steady state velocity as *incubation* period, t_i at a field E_0. At E_0, if the wall moved a distance x by applying a voltage pulse of width t_w, then the velocity measurements of Ref. 4 and this work will be x/t_w and $x/(t_w-t_i)$, respectively. From this work, we would then estimate the ratio of the velocities to be $t_w/(t_w-t_i)\sim 10$ which would mean that the incubation time $t_i=0.9t_w$ in Ref. 4 at the field corresponding to a switching time of ~1 s. Obviously, if we increase the pulse width to a very large one, (tending toward a step voltage, $t_w\rightarrow\infty$), the pulse voltage velocity measurements would become larger since the incubation time would become much smaller than the pulse width. This also means that if the frequency of voltage pulsing were increased to much greater than 1–2 pulse per second, then the pulsed voltage measurements and real-time step voltage measurements would yield similar results for wall velocity.

We are currently re-examining these aspects using EOIM. These observations are particularly important since most of the domain wall velocity measurements in the literature on various ferroelectric crystals have been performed by pulse voltage experiments.[6–8]

B. Merger of domain walls

The ''speeding up'' of domains on forming a merged front like that in Fig. 6 is another significant observation. For the same field value, a merged domain front moves an order of magnitude faster than independently growing domain triangles. In this study, we can observe this effect by comparing Figs. 5 and 6.

We propose a simple qualitative model to explain the essence of this behavior. Figure 9 shows a schematic of the intersection of two growing 180° domain triangles to form a ledge. Following the argument of Miller and Weinreich,[14] further growth of domain walls will occur by preferential nucleation at the domain wall. Assuming that the nuclei also possess the same triangular symmetry of the larger domains in the Z plane, one can write the change in free energy (ΔU_{3D}) in three dimensions (3D) due to the formation of a nucleus as

$$\Delta U_{3D}=-2P_sE\Delta V_{3D}+\sigma_w\Delta A_{3D}+U_d, \qquad (2)$$

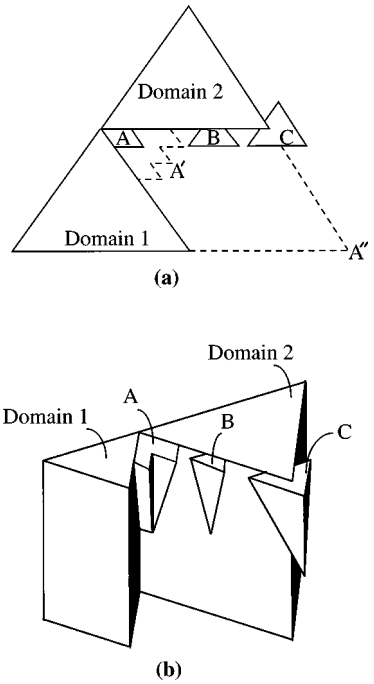

FIG. 9. Schematic of possible nucleation sites upon merger in (a) 2D case and (b) a 3D case. Of the three possible nucleation sites, A, B, and C, nucleus A at the ledge is the most preferred since it involves no net change in the domain wall length before and after nucleation. This nucleus will propagate out as front A′ with a higher sideways velocity until it reaches the larger triangle A″ (both shown in broken lines).

where P_s is the spontaneous polarization, E is the external electric field, ΔV_{3D} is the volume of the nucleus, σ_w is the wall energy per unit area, ΔA_{3D} is the change in wall area due to the nucleus, and U_d is the depolarization energy. The first term in Eq. (2) is the decrease in the volume electrostatic energy, the second term is the net increase in domain wall energy, and the third term is the increase due to depolarization energy.

Let us first consider the energy change ΔU_{2D}, in a simple two-dimensional (2D) picture of merger as shown in Fig. 9(a). In this 2D picture, we can for the moment ignore the depolarization energy, U_d in Eq. (2). The volume change, ΔV_{3D}, in Eq. (2) can, accordingly, be replaced by an area change, ΔA_{2D}, in the Z plane (the plane perpendicular to the polarization axis), and the wall area change ΔA_{3D} can be replaced by the wall length change ΔL_{2D}. By comparing nuclei A and B (or C), one can immediately deduce that for a fixed area of the nuclei ΔA_{2D}, the domain lengths change, $\Delta L_{2D}=0$ for nucleus A and $\Delta L_{2D}>0$ for nuclei B and C. Thus the energy changes $(\Delta U_{2D})_A<(\Delta U_{2D})_B$ or $(\Delta U_{2D})_C$. In other words, in this 2D picture, the formation of nucleus A lowers the electrostatic energy, but costs no more in additional energy for the formation of domain walls, since the net wall length remains the same. This is true for any nucleation at the ledge similar to nucleus A, but with various levels of serration to the wall front, depicted, for example by the broken lines of wall A′ in Fig. 9(a). This is, however, not true for nucleation at sites B or C, where there will be a significant increase in the domain wall length. Thus, upon the merging of triangular domain walls, ledges are formed at the

intersection of these domains. These domains have a much stronger driving force for nucleation than the flat walls of an independently growing domain. The merged domain front in Fig. 9 will speed up until it reaches the dotted line, A″, where the ledge disappears. Further growth from this point onward will be at a lower steady state velocity like that of domains I and II in Fig. 5.

We must point out that in this 2D case, $(\Delta U_{2D})_A = -2P_sE\Delta A_{2D} < 0$. A steady state velocity, of the form $v_s \propto \exp(-(\Delta U_{2D})/kT)$,[14] is no longer physical since it would suggest that, at zero field, v_s is nonzero. Instead, a merged domain front such as A or A′ should accelerate at a constant field under a force $-\partial U/\partial y$ where the coordinate y is normal to the domain walls. This is contrary to the steady state velocity observed in Fig. 6. Let us consider the more realistic three-dimensional case depicted in Fig. 9(b). The nuclei initially form daggers in the thickness direction of the *Z*-cut crystal. The net area change of the domain wall, ΔA_{3D}, is not exactly zero for nucleus A anymore since the new wall segments are not necessarily parallel to the old walls in the planes parallel to the polarization direction. Further, one can no longer neglect the depolarization energy U_d in Eq. (2). However, one still retains the essence of the argument presented for the 2D case if the dagger shaped nuclei have a very large aspect ratio, i.e., much longer in the polarization direction than they are wide in the *Z* plane. This is indeed observed since this aspect ratio has been reported earlier to be ~14 for $LiTaO_3$.[4] This implies that ΔA_{3D}, although finite, is very small for nucleus A and significantly larger for nuclei B and C. We now believe that one also needs to take into account additional frictional energy terms due to pinning mechanisms active during domain wall motion. Taking these changes into account, one could expect to obtain $(\Delta U_{2D})_A$ to be small but positive, which could account for an increased steady state velocity v_s at a constant field.

C. Residual traces behind a moving wall

Another interesting observation is evident in the electro-optic video images of the domain walls in Fig. 4. Inside a growing domain, one observes shadows or traces of previous positions of the domain wall. This is most clearly seen in the merged domain fronts. Figure 10 shows an expanded version of a section of frame (i) in Fig. 4 to illustrate this point. The traces are indicated by arrow heads. These traces disappear with time in ~0.1–1 s, and, since every frame in video is 1/30 s apart, these traces are therefore captured in real-time imaging. The time constant for the disappearance immediately suggests a possible connection to the stabilization time of a domain wall in $LiTaO_3$ which is ~1 s. We presently believe that this residual contrast is associated with a strain field associated with the domain wall. It was reported earlier that a 180° domain wall in congruent $LiTaO_3$ is associated with birefringence[5] and a strain field.[11] These features also show strong correlation to internal fields,[5] which in turn arise from lithium nonstoichiometry in the crystals.[10] Although it is not clear exactly how the point defects give rise to macroscopic strains and birefringence, one can say that when a domain wall moves in the crystal, the strain field associated with the wall should tend to disappear at the original location of the domain wall and reform at the new location. We believe that it is this process of disappearance of strain fields which we see as the disappearance of traces behind a leading domain wall front. We must point out that the fading residual traces behind a moving domain wall cannot have their origin in the electro-optic effect due to external field, since a domain wall no longer exists at the site of a trace. This contrast is most likely related to residual internal strains which relax with time.

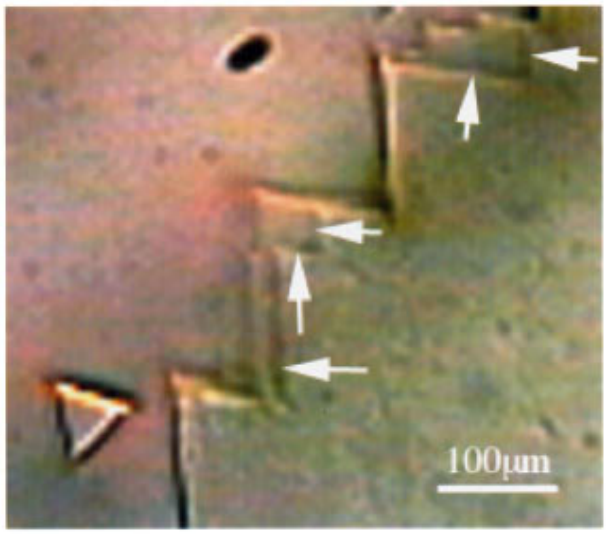

FIG. 10. Transient traces left behind a moving domain wall in congruent $LiTaO_3$ are indicated by arrow heads. These traces disappear with time ~0.1–1 s. This area is an expanded view of a section of Fig. 4(i).

V. CONCLUSIONS

We have imaged the nucleation and growth of ferroelectric 180° domains in $LiTaO_3$ in real time using electro-optic imaging microscopy. Two important observations were made possible by this *in situ* technique. The first is that the sideways wall velocities of domain walls under an external field are an order of magnitude larger than those previously reported by pulsed voltage application followed by *ex situ* observation. The second is that we have been able to study the merging kinetics of growing domain walls, and observe a further order of magnitude increase in domain wall velocities upon domain merger. We attribute this to formation of ledges upon the merger where preferential domain nucleation occurs. Further studies on the field dependence of wall velocities and nucleation rates are in progress.

ACKNOWLEDGMENTS

This work was supported by the U.S. Department of Energy, Office of Basic Energy Science, and by a director funded postdoctoral fellowship at Los Alamos National Laboratory.

[1] V. Gopalan, M. Kawas, T. E. Schlesinger, M. C. Gupta, and D. D. Stancil, IEEE Photonics Technol. Lett. **8**, 1704 (1996).
[2] V. V. Lemanov and Yu. V. Lisavsky, Ferroelectrics **42**, 77 (1982).

[3] S. Breer, K. Buse, K. Peithmann, H. Vogt, E. Kratzig, Rev. Sci. Instrum. **69**, 1591 (1998).
[4] V. Gopalan and T. E. Mitchell, J. Appl. Phys. **83**, 941 (1998).
[5] V. Gopalan and M. C. Gupta, J. Appl. Phys. **80**, 6099 (1996).
[6] W. J. Merz, Phys. Rev. **95**, 690 (1954).
[7] R. C. Miller and A. Savage, Phys. Rev. **115**, 1176 (1959).
[8] E. G. Fesenkp, A. F. Semenchev, and V. G. Gavrilyatchenko, J. Appl. Phys. **34**, 3255 (1963).
[9] K. Onuki, N. Uchida, and T. Saku, J. Opt. Soc. Am. **62**, 1030 (1972).
[10] V. Gopalan, T. E. Mitchell, Y. Furukawa, and K. Kitamura, Appl. Phys. Lett. **72**, 1981 (1998).
[11] T. J. Yang, U. Mohideen, and M. C. Gupta, Appl. Phys. Lett. **71**, 1960 (1997).
[12] T. J. Yang and U. Mohideen, Phys. Lett. A (in press).
[13] T. J. Yang, U. Mohideen, V. Gopalan, and P. Swart (unpublished).
[14] R. C. Miller and G. Weinreich, Phys. Rev. **117**, 1460 (1960).